

# Noise Recycling

Alejandro Cohen\*, Amit Solomon\*, Ken R. Duffy†, and Muriel Médard\*

\*RLE, MIT Cambridge, MA 02139, USA, {cohenale,amitsol,medard}@mit.edu

†Hamilton Institute Maynooth University, Ireland, ken.duffy@mu.ie

**Abstract**—We introduce Noise Recycling, a method that substantially enhances decoding performance of orthogonal channels subject to correlated noise without the need for joint encoding or decoding. The method can be used with any combination of codes, code-rates and decoding techniques. In the approach, a continuous realization of noise is estimated from a lead channel by subtracting its decoded output from its received signal. The estimate is recycled to reduce the Signal to Noise Ratio (SNR) of an orthogonal channel that is experiencing correlated noise and so improve the accuracy of its decoding. In this design, channels only aid each other only through the provision of noise estimates post-decoding.

For a system with arbitrary noise correlation between orthogonal channels experiencing potentially distinct conditions, we introduce an algorithm that determines a static decoding order that maximizes total effective SNR with Noise Recycling. We prove that this solution results in higher effective SNR than independent decoding, which in turn leads to a larger rate region. When the noise is jointly Gaussian, we establish that Noise Recycling employing this static successive order enables higher code rates. We derive upper and lower bounds on the capacity of any sequential decoding of orthogonal channels with correlated noise where the encoders are independent and show that those bounds are almost tight. We numerically compare the upper bound with the capacity of jointly Gaussian noise channel with joint encoding and decoding, showing that they match.

Simulation results illustrate that Noise Recycling can be employed with any combination of codes and decoders, and that it gives significant Block Error Rate (BLER) benefits when applying the static predetermined order used to enhance the rate region. We further establish that an additional BLER improvement is possible through Dynamic Noise Recycling, where the lead channel is not pre-determined but is chosen on-the-fly based on which decoder provides the most confident decoding. Noise Recycling thus offers significant decoding performance improvements without the need for specific codes and decoders, or additional coordination between the sender and receiver.

**Index Terms**—Noise Recycling, FEC, Channel Decoding, Correlated Noise, Orthogonal Channels.

## I. INTRODUCTION

The use of orthogonal channels is commonplace in applications from wired to wireless channels. Examples include the wide-spread use of orthogonal frequency division multiplexing (OFDM) [2]–[4], and of orthogonal schemes in multiple access, such frequency division multiplexing access (FDMA), time-division multiple access (TDMA), or orthogonal code-division multiple access (CDMA), see, for instance [5]. Let us consider the case of adjacent channels in a fading channel environment, for instance in OFDM or TDM. In OFDM (TDM), channels or (channel uses) separated by less than a coherence

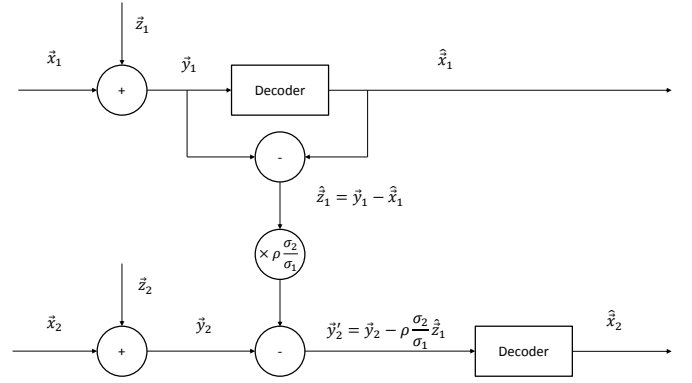


Fig. 1: In Noise Recycling, a noise estimate is created from a lead channel by subtracting its modulated decoding from the received signal. That estimate is used to reduce noise on a channel subject to correlated noise prior to decoding.

band (coherence time) will experience correlated fading [6]–[11], or equivalently, correlated noise. While in theory joint decoding across channels can make use of such correlation to improve performance [12], [13], in practice it is a challenge to implement owing to the computation complexity of the decoding, and lack of compatibility with existing decoding schemes. Indeed, joint decoding runs counter to the reason for seeking orthogonality in the first place.

Here we introduce a novel approach, Noise Recycling, that embraces noise correlation to significantly improve decoding performance while maintaining separate encoding and decoding across distinct channels. The scheme is compatible with all encoding and decoding schemes, and requires no coordination between channels. Its underlying principle is that the realisation of noise experienced on that channel is revealed when a decoding is correct, and that information can be used to reduce the effective SNR for a neighbouring communication.

Fig. 1 provides an illustration of the technique. Two independent channel inputs,  $(\bar{x}_1, \bar{x}_2)$ , from potentially different codebooks are transmitted on orthogonal channels and are corrupted by real-valued, mean-zero noise  $(\bar{Z}_1, \bar{Z}_2)$  with correlation  $\rho$  and variances  $\sigma_1^2$  and  $\sigma_2^2$ . This results in correlated random real-valued channel outputs  $(\bar{Y}_1, \bar{Y}_2) = (\bar{x}_1, \bar{x}_2) + (\bar{Z}_1, \bar{Z}_2)$ . For a particular realization of outputs,  $(\bar{y}_1, \bar{y}_2)$ , a lead channel is selected, say channel 1, and  $\bar{y}_1$  is decoded to give  $\hat{x}_1$ . The decoder then estimates the noise realization experienced on the lead channel by subtracting the decoded codeword from the received signal  $\hat{z}_1 = \bar{y}_1 - \hat{x}_1$ . This noise estimate is recycled to the second receiver who updates its channel output prior to decoding via the Linear Least Square Estimator:  $\bar{y}'_2 = \bar{y}_2 - \rho \sigma_2 / \sigma_1 \hat{z}_1$ . If the lead decoding is correct,

Parts of this work [1] were presented at the IEEE International Symposium on Information Theory, ISIT 2020.

which happens with probability one minus the BLER, this eliminates part of the additive noise experienced on the second channel  $\vec{z}_2$ , before decoding, Noise Recycling results in the revised second channel's output being a less noisy version of the channel input  $\vec{x}_2$ , which in turn leads to improved decoding performance.

For code-rates below capacity, in the large code-length limit concentration onto correct decodings occurs. This ensures that Noise Recycling enables a larger rate region than independent decoding. For BLER, there is a trade-off between the improved SNR that comes with correct recycled noise and the disadvantage of passing an erroneous estimate. A heuristic argument for why a gain is to be expected is as follows. Consider two channels that have a block error rate curves  $B(\cdot)$  that is an increasing function of their noise variance  $\sigma^2$  when they are decoded independently, and assume that they experience noise with correlation  $\rho$ . Suppose that the lead decoder either decodes correctly or flags an error, as is the case in systems using a CRC post-decoding for decoding validation. With probability  $B(\sigma^2)$  the lead channel would offer no noise for recycling and the BLER performance of the second channel would also be  $B(\sigma^2)$ . If the lead channel decoded correctly, which occurs with probability  $1 - B(\sigma^2)$ , the second channel would experience a BLER of  $B(\sigma^2(1 - \rho^2))$ , giving, on average,

$$B(\sigma^2)B(\sigma^2) + (1 - B(\sigma^2)) B(\sigma^2(1 - \rho^2)) < B(\sigma^2). \quad (1)$$

Thus if the lead decoder never decodes erroneously, recycling is always advantageous. Even in the absence of codeword validation post-decoding, as errors are, in practice, rare, the benefits of Noise Recycling are typically significant.

Noise Recycling is distinct from Interference Cancellation in multiple access channels, where decoded codewords are subtracted from received signals to remove interference [5], [12], [14], [15]. In Noise Recycling modulated decoded codewords are subtracted from received signals to recover noise estimates which, owing to correlation across channels, form a component of the noise in another as-yet undecoded orthogonal channel. A proportion of the estimate can, therefore, be subtracted from the received signal on the orthogonal channel before decoding, reducing the latter's effective noise. In non-orthogonal channels subject to both interference and correlated noise, Noise Recycling and Interference Cancellation could be used together.

In Section III we mathematically establish the rate gain that Noise Recycling provides over independently decoding the channels. In Section III-A we provide an algorithm based on Maximum Directed Spanning Tree (MDST) that finds an optimal static Noise Recycling decoding order for arbitrarily correlated orthogonal channels in terms of maximizing the sum of effective SNR. Assuming the noise is jointly Gaussian, in Section III-B we identify the extent of the enhanced rate region that is made possible by the improved effective SNR. We numerically evaluate rate gains over independent decoding of channels, finding they improve both as correlation increases and as the number of orthogonal channels increases for a given correlation. For jointly Gaussian noise we then provide an upper bound on the capacity of any pair of orthogonal channels

with correlated noise in Section III-C. We compare the upper bound with the achievability rate region given in Section III-B for Noise Recycling, finding that these bounds essentially coincide. This upper bound is numerically compared to the capacity of the channel using joint decoding in which the encoders may cooperate [12, Section 9.5] [16], [17] and, for the model considered in this work, the upper bound and the capacity of the channel match.

In Section IV, through simulation we determine the BLER improvements yielded by Noise Recycling. We illustrate that Noise Recycling can provide performance gains with any codes at any rates using any decoders. We consider two distinct settings. The one in Section IV-A is similar in spirit to the approach presented in Section III and employs the static channel recycling order that is determined based on channel statistics via the MDST. The second setting, Section IV-B, does not use a pre-determined decoding order, but instead a dynamic per-realization one. The decoders of orthogonal channels are first run in parallel. The decoding that results in the most confident decoding provides the first estimate for Noise Recycling. While this approach is not designed to provide rate gains, we show that it yields considerable BLER improvements for both short and long codes. Finally, we also consider the possibility of re-recycling, where the lead channel is itself fed a recycled noise estimate, finding that this bootstrapping can improve the BLER performance of the leading channel. A heuristic argument is provided in support of that observation.

## II. SYSTEM MODEL

Let  $x, \vec{x}, X, \vec{X}$  denote a scalar, vector, random variable, and random vector, respectively. All vectors are row vectors. A linear block code is characterized by  $[n, k]$ , a code-length,  $n$ , and a code-dimension,  $k$ , giving a rate  $R = k/n$ . The binary field is denoted by  $\mathbb{F}_2$ . Mutual information between  $X, Y$  is denoted by  $I(X; Y)$ .

We study an orthogonal channel system where  $i \in \{1, \dots, m\}$  messages,  $\vec{u}_i \in \mathbb{F}_2^{k_i}$ , are encoded into codewords  $\vec{c}_i \in \mathbb{F}_2^n$ . Each codeword is modulated into a block  $\vec{x}_i$  of real values and sent over continuous orthogonal channels subject to additive real-valued noise. Channel outputs are

$$\vec{Y}_i = \vec{x}_i + \vec{Z}_i,$$

where,  $Z_i(l)$  the  $l$ -th element of  $\vec{Z}_i$ , has mean zero and variance  $\sigma_i^2$ . For each  $(i, j)$ -th pair of orthogonal channels the noise  $(Z_i(l), Z_j(l))$  is assumed to follow a joint distribution with correlation

$$\rho_{i,j} = \frac{\mathbb{E}(Z_i(l)Z_j(l))}{\sigma_i\sigma_j}, \text{ where } \rho'_{i,j} = \rho_{i,j} \frac{\sigma_j}{\sigma_i}$$

denotes the normalized correlation factor of the  $j$ -th channel that is used in the linear least square estimator (LLSE) for  $Z_j(l)$  given  $Z_i(l)$ . The rate of the  $i$ -th code is  $R_i = k_i/n$ , and the total rate is  $R = \sum_{i=1}^m R_i$ . Given  $(\vec{Y}_1, \dots, \vec{Y}_m)$ , the goal is to estimate  $(\vec{c}_1, \dots, \vec{c}_m)$  using  $m$  distinct decoders.

When considering rate regions, we assume that each channel is decoded only once. As a result, the SNR of the lead

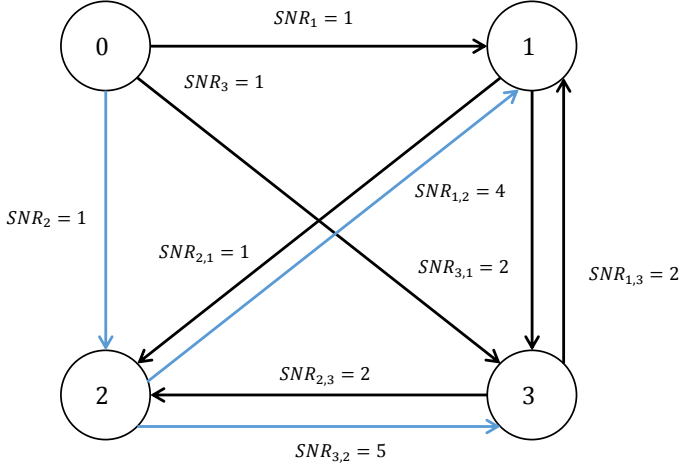


Fig. 2: An example of the constructed graph of Section III-A. There are  $m = 3$  orthogonal channels. The edges of a Maximum Directed Spanning Tree are painted in blue. In this example, the leading channel is the second orthogonal channel. The estimation of the second orthogonal channel is sent to the first and third orthogonal channels.

channel remains unchanged. In the simulation results, however, we consider circumstances where the decoders may operate repeatedly.

### III. EFFECTIVE SNR GAIN WITH NOISE RECYCLING

In this section we determine the rate region that can be achieved by using Noise Recycling. We show that the total effective SNR increases when Noise Recycling is applied. When Noise Recycling is not used, each orthogonal channel has to be decoded independently with a rate below that channel's capacity. In Noise Recycling, we update the received signal of the  $j$ -th channel using noise estimated from the  $i$ -th channel's decoding via the linear least squared estimator

$$Y_j' = Y_j - \rho_{i,j}' Z_i = X_j + Z_j - \rho_{i,j}' \frac{\sigma_j}{\sigma_i} Z_i.$$

To see that it increases effective SNR with the recycled noise is correct, note that

$$\text{var}(Z_j - \rho_{i,j}' Z_i) = \text{var}(Z_j) (1 - \rho_{i,j}^2), \quad (2)$$

and this is less than  $\text{var}(Z_j)$  so long as  $\rho_{i,j}^2 > 0$ . As a result, Noise Recycling increases the orthogonal channel's effective SNR when the recycled noise is correct. When the channel noise variances,  $\text{var}(Z_j)$ , are heterogeneous, eq. (2) demonstrates that Noise Recycling impacts SNR in an asymmetric manner and so the order in which noise is recycled impacts the total effective SNR.

#### A. Optimal Decoding Order

We identify a solution to the problem of determining an optimal static order for Noise Recycling using tools from graph theory. We first construct an almost fully connected directed graph  $\mathcal{G} = (\mathcal{V}, \mathcal{E})$  with  $m + 1$  nodes. Each node represents an orthogonal channel, with one additional node

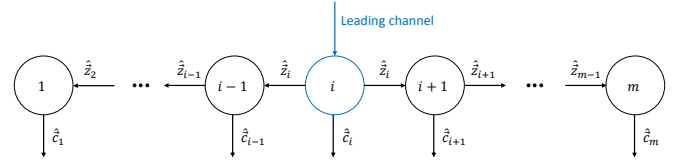


Fig. 3: Gauss-Markov noise model, where correlation between adjacent orthogonal channels is  $\rho$ . A leading orthogonal channel  $i$  is decoded first, and propagation of noise estimations follows to help decoding of all orthogonal channels.

called the zero node.  $\mathcal{G}$  contains a directed edge from every node to every node, with the exception of the zero node, which has only outgoing edges to all other nodes. Each edge  $(i, j)$  is associated with a weight

$$w_{i,j} = \begin{cases} \text{SNR}_{i,j} & i \neq 0, j \neq 0 \\ \text{SNR}_j & i = 0 \end{cases},$$

where  $\text{SNR}_{i,j}$  is the effective SNR of orthogonal channel  $i$  when using noise recycled estimation of orthogonal channel  $j$ , and  $\text{SNR}_j$  is the SNR of orthogonal channel  $j$  without Noise Recycling. Recall that  $\text{SNR}_{i,j}$  is a function of the transmission power on channel  $i$ , the statistics of the noise in channel  $i$ ,  $\sigma_i$ , and the correlation factor  $\rho_{i,j}'$ . The zero nodes helps us represent the SNR associated with decoding without Noise Recycling. An example of such graph with  $m = 3$  is shown in Fig. 2.

We show a decoding order which uses a MDST. Finding a MDST can be done efficiently using Edmond's algorithm [18]. Recall that a MDST  $\mathcal{G}' = (\mathcal{V}', \mathcal{E}')$ , with a root node  $r \in \mathcal{V}$ , has the following properties:

- 1)  $\mathcal{V}' = \mathcal{V}, \mathcal{E}' \subseteq \mathcal{E}$ .
- 2)  $\forall i \in \mathcal{V}', i \neq r : \exists$  a path from  $r$  to  $i$  in  $\mathcal{E}'$ .
- 3) The undirected version of  $\mathcal{G}'$  is a tree.
- 4) The cost of  $\mathcal{G}'$ , which is defined as the sum of all the weights of  $\mathcal{E}'$ , is maximal among all possible Directed Spanning Trees of  $\mathcal{G}$ .

The decoding order we propose traverses a MDST of  $\mathcal{G}$  in a Breadth First Search (BFS) fashion [19] (although other tree traversals are possible): First, all the nodes that are connected to the zero node in  $\mathcal{G}'$  are decoded without noise recycling. Then, every node that is connected to a previously decoded node is decoded, using the noise recycled estimation of its parent node. In the example of Fig. 2, only node number 2 is connected to the zero node in the MDST. Hence, only orthogonal channel number 2 is decoded without Noise Recycling. Then, orthogonal channels number 1 and 3 are decoded with Noise Recycling, using the estimation of the noise of the second orthogonal channel, as dictated by the MDST. We see that the sum of the SNR with Noise Recycling is  $1 + 4 + 5$ , which is the highest possible sum in this example, as opposed to  $1 + 1 + 1$  without Noise Recycling. Later in this section, we show in Theorem III.2 that the achievable rates of this example are  $C(1), C(4), C(5)$ , unlike  $C(1), C(1), C(1)$  without Noise Recycling, where  $C(\cdot)$  is the capacity of the underlying channel as a function of SNR. Pseudo-code of the

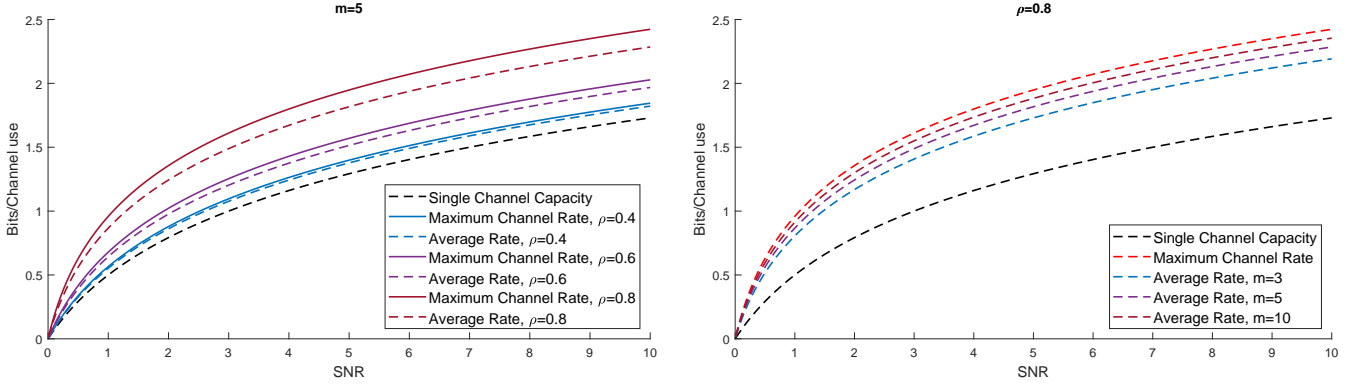


Fig. 4: Achievable regime for the decoder of Section III. Single Channel Capacity is  $C_1 = C(P/\sigma^2) = 1/2 \log(1 + P/\sigma^2)$ , the capacity of an orthogonal channel that does not use recycled noise, as is the case for the first channel,  $j = 1$ . Maximum Channel Rate is the rate of an orthogonal channel decoded with Noise Recycling  $C_j = C(P/((1 - \rho^2)\sigma^2))$ ,  $j > 1$ . The average rate is the average rate per orthogonal channel, namely  $(C_1 + (m - 1)C_2)/m$ .

procedure is given in Algorithm 1. Note that lines 8,10 use the channel output  $\vec{y}_j$ , and  $\hat{z}_i, \rho'_{i,j}$  in line 10. We prove that this solution is optimal for finding a decoding order which maximizes the sum of SNRs:

---

#### Algorithm 1 Noise Recycling Order

---

**Input:**  $\vec{y}_1, \dots, \vec{y}_m$

**Output:**  $\hat{c}_1, \dots, \hat{c}_m$

```

1:  $\mathcal{G} \leftarrow$  almost fully connected directed graph of Section III-A
2:  $\mathcal{G}' \leftarrow$  MDST of  $\mathcal{G}$ 
3:  $\mathcal{N} \leftarrow \{r\}$  ▷ BFS queue
4: while  $\mathcal{N} \neq \emptyset$  do
5:    $i \leftarrow \text{pop}(\mathcal{N})$  ▷ Extract the head of  $\mathcal{N}$ 
6:   for all  $j$  s.t.  $(i, j) \in \mathcal{E}'$  do
7:     if  $i = r$  then
8:        $\hat{c}_j \leftarrow$  Decode  $j$  without Noise Recycling
9:     else
10:       $\hat{c}_j \leftarrow$  Decode  $j$  with Noise Recycling of  $i$ 
11:    end if
12:    Add  $(\mathcal{N}, j)$  ▷ Add  $j$  to the end of  $\mathcal{N}$ 
13:  end for
14: end while

```

---

**Lemma III.1.** For arbitrary channels with arbitrary correlation  $\rho_{i,j}$  between orthogonal channels  $i, j$ , Algorithm 1 determines an order that maximizes the sum of effective SNR when every orthogonal channel is decoded once.

*Proof.* The proof stems directly from the properties of a MDST. We have to prove the following:

- 1) At least one channel is decoded without Noise Recycling.
- 2) Each orthogonal channel is decoded exactly once.
- 3) The decoding order yields maximum total SNR.

Property 1 is satisfied as  $r$  has at least one outgoing edge in  $\mathcal{G}'$ , as a path from  $r$  to  $i$  exists for every  $i \neq r$ . Property 2 is satisfied as  $\mathcal{G}'$  is a Directed Spanning Tree; Every node is

reached, and no node can be reached more than once, as a tree has no cycles. Property 3 follows by the definition of a MDST.  $\square$

#### B. Achievable Region

While Lemma III.1 holds in general, we present the main theorem for jointly Gaussian noise. By improving the effective SNR, a larger rate region is achievable than in the case where Noise Recycling is not used.

**Theorem III.2.** Assume a noise model with fixed  $m$  orthogonal jointly Gaussian channels, each with variance  $\sigma_j^2$ . For a given average power constraint,  $\mathbb{E}(X_j^2) \leq P_j$ , and any correlation factor  $|\rho_j| < 1$ , the following region is achievable:

$$R_j < C \left( \frac{P_j}{(1 - \rho_j^2)\sigma_j^2} \right)$$

where

$$\rho_j = \begin{cases} \rho_{\pi(j),j} & \pi(j) \neq r \\ 0 & \pi(j) = r \end{cases},$$

$r$  is the root of the MDST (the zero node),  $\pi(j)$  is the parent of  $j$  in the MDST,  $P_j/\sigma_j^2$  is the SNR and  $C(P_j/\sigma_j^2) = 1/2 \log(1 + P_j/\sigma_j^2)$  is the resulting capacity.

*Proof.* The proof is given in Appendix A.  $\square$

Note that in the case of joint Gaussianity, the  $j$ -th noise vector  $\vec{Z}_j$  can be generated in the following way,  $Z_j(l) = \rho'_{i,j} Z_i(l) + \Xi_{i,j}(l)$ , where  $Z_i(l) \sim \mathcal{N}(0, \sigma^2)$  and  $\Xi_{i,j}(l) \sim \mathcal{N}(0, (1 - \rho^2)\sigma^2)$  are independent Gaussians.

The Gauss-Markov (GM) process has been used to model progressive decorrelation of fading with growing separation among channels [20]–[25] in time, frequency, or both, according to, say, Jakes's model [26]. Mapping fading to an equivalent noise model leads naturally to a GM model of noise [27]–[34] to represent these effects.

**Corollary III.2.1.** When the noise is GM, i.e. a symmetric multivariate Gaussian with  $\sigma_j = \sigma$ ,  $\rho_{i,j} = \rho^{|i-j|}$ , and equal

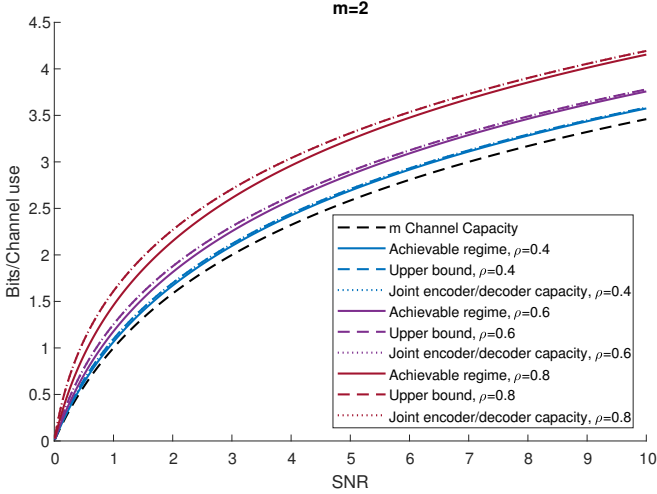


Fig. 5: Upper bound vs. achievable regime for  $m = 2$  orthogonal channel. The capacity of  $m$  channels is  $C_m = m \cdot C(P/\sigma^2)$ . Achievable regime is the sum rate using Theorem III.2. Upper bound is the sum rate using the bound given in Theorem III.3. The cross channel joint encoder-decoder channel capacity is  $C_m = \max_{\frac{1}{m} \text{tr}(\Lambda_{\underline{X}}) \leq P} \frac{1}{2} \log \left( \frac{|\Lambda_{\underline{X}} + \Lambda_{\underline{Z}}|}{|\Lambda_{\underline{Z}}|} \right)$ , where  $\Lambda_{\underline{X}}$  is the cross-correlation matrix of the input energies and  $\Lambda_{\underline{Z}}$  is the cross-correlation matrix of the correlated noise, see [12, Section 9.5].

average transmission power constraint  $P_j = P$ , we get the following result:  $\pi(j) = j - 1$  (where the root  $r$  is the zero node) and the achievable rates are

$$R_1 < C \left( \frac{P}{\sigma^2} \right), \quad R_j < C \left( \frac{P}{(1 - \rho^2) \sigma^2} \right), \quad \text{for all } j > 1,$$

where  $P/\sigma^2$  is the SNR and  $C(P/\sigma^2) = 1/2 \log(1 + P/\sigma^2)$  is the capacity.

The decoding order of a GM model is shown in Fig. 3 where the leading channel is  $i = 1$ . The achievable rates are depicted in Fig. 4, which illustrates the rate that can be gained by Noise Recycling when compared to the case where channel decoders operate independently. It is evident that there is a gap between the single-channel capacity and the average rate that can be achieved by decoders employing Noise Recycling. In particular, there is a significant rate-gain even when the number of orthogonal channels,  $m$ , or the noise correlation,  $|\rho|$ , is low.

We comment that Theorem III.2 can be naturally expanded to FDMA and TDMA, where the rates have to be adjusted as in [12, Chapter 15.3.6].

### C. Upper Bound on Rate Region

We now provide an upper bound on the rate region for orthogonal channels with noise correlation  $\rho_{i,j}$  in order to determine what, if anything, is lost by our use of independent decoders with Noise Recycling when compared with joint encoding and decoding. Fig. 5 shows the upper bound rate region given in Theorem III.3 (below). Moreover, we compare

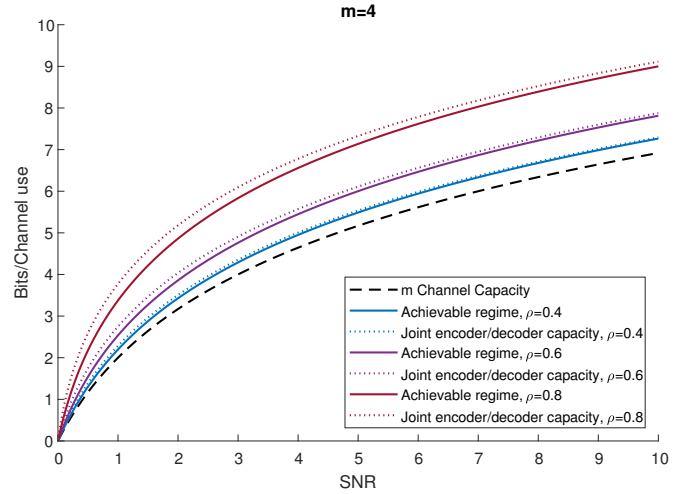


Fig. 6: Capacity and achievable region for  $m = 4$ . We see that the achievable region is still close to the capacity, even when the number of channels increase.

the upper bound to the achievable regime using the Noise Recycling decoding scheme provided in Theorem III.2, the case where channel decoders operate independently as given in [12, Section 9.4], and the case where the encoders may cooperate and there is a joint decoder as given in [12, Section 9.5].

For a GM model, it is evident from the comparison presented in Fig. 5 that there is a small gap that increases with  $\rho$  between the upper bound and the achievable regime using the proposed Noise Recycling scheme. Yet, we note that for noise correlation lower than 0.6 or for SNRs higher than 6, the bounds almost match. Furthermore, it is important to note that the upper bound provided in this section for the case that the encoders are independent, as considered in this paper, match the capacity of the model where the encoders may cooperate and there is a joint decoder. Recall that we consider a model where  $Z_j \sim \mathcal{N}(0, \sigma^2)$  for each  $j$ -th orthogonal channel, as given in Section II.

**Theorem III.3.** Assume a correlated noise model with fixed  $m$  orthogonal channels, each with variance  $\sigma_j^2$ , and correlation  $\rho_{i,j}$  between each  $(i, j)$  pair of orthogonal channels. For independent encoders with a given average power constraint,  $\mathbb{E}(X_j^2) \leq P_j$ , and any correlation factor  $|\rho_{i,j}| < 1$ , the capacity of any pair of orthogonal channels is upper bounded by,

$$C \leq \frac{1}{2} \log \left( 1 + \frac{P_i}{\sigma_i^2} \right) + \frac{1}{2} \log \left( \frac{P_j + \sigma_j^2}{P_j + (1 - \rho_{i,j}^2) \sigma_j^2} \right) + \frac{1}{2} \log (1 - \tilde{\rho}_{i,j}^2) + \frac{1}{2} \log \left( 1 + \frac{P_j}{(1 - \rho_{i,j}^2) \sigma_j^2} \right),$$

where

$$\tilde{\rho}_{i,j} = \rho_{i,j} \frac{\sigma_i \sigma_j}{\sqrt{(P_i + \sigma_i)(P_j + \sigma_j)}}.$$

*Proof:* The proof is given in Appendix B.



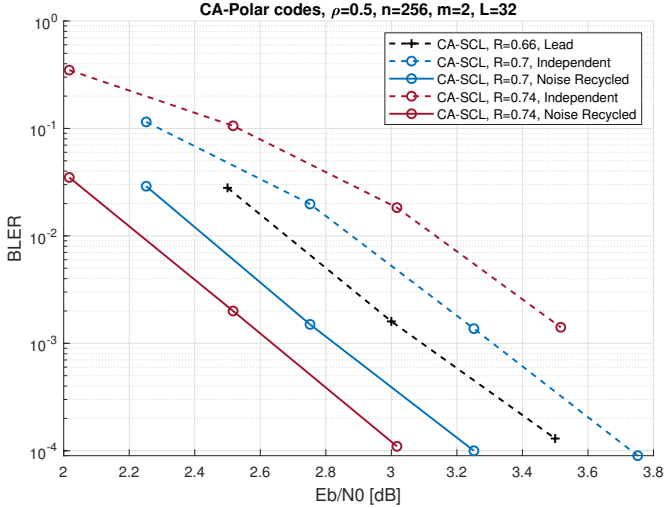


Fig. 7: BLER vs.  $E_b/N_0$  for 256 bit CA-Polar codes decoded with CA-SCL, uses a list size of  $L = 32$ , with and without Noise Recycling. Dashed lines correspond to independent decoding, and solid lines to decoding after Noise Recycling. The lead orthogonal channel is encoded with a rate  $2/3$  code. The second channel uses either a rate 0.7 or 0.74 code.

The upper bound provided in Theorem III.3 is for any pair of orthogonal channels. Yet we note from Fig. 6 that the same trend concerning the tightness of the bounds is maintained when the number of orthogonal channels increases, comparing the achievable regime using Noise Recycling to the capacity with encoders that may cooperate and a joint decoder is used.

#### IV. NOISE RECYCLING BLER IMPROVEMENT

In Section III we determined the rate-gains available from Noise Recycling through the use of random codebooks and joint typicality. Here we illustrate that BLER performance can be enhanced by Noise Recycling when used with existing codes and decoders. Simulations employ a jointly Gaussian channel model with Binary Phase Shift Keying (BPSK) modulation. We demonstrate the technique with a diverse range of codes and decoders in terms of sizes and rates to illustrate the general utility of the method.

For codes, we use:

- CRC-Aided Polar (CA-Polar) Codes [35], [36], which are Polar codes [37], [38] with an outer CRC code. These have been proposed for all control channel communications in 5G NR [39].
- Low Density Parity Check (LDPC) codes [40], which have been proposed for all data channel communications in 5G NR [39] and typically have long code-lengths.
- Random Linear Codes (RLCs), which have long-since been known to be capacity achieving [41], but have been little investigated owing to the lack of availability of decoders until the recent development of Guessing Random Additive Noise Decoding (GRAND) [42]–[45].

For decoders, we use the state-of-the-art CA-Polar-specific CRC-Aided Successive Cancellation List decoder (CA-SCL) [35], [36], [46]–[48] and the LDPC decoder using Belief Prop-

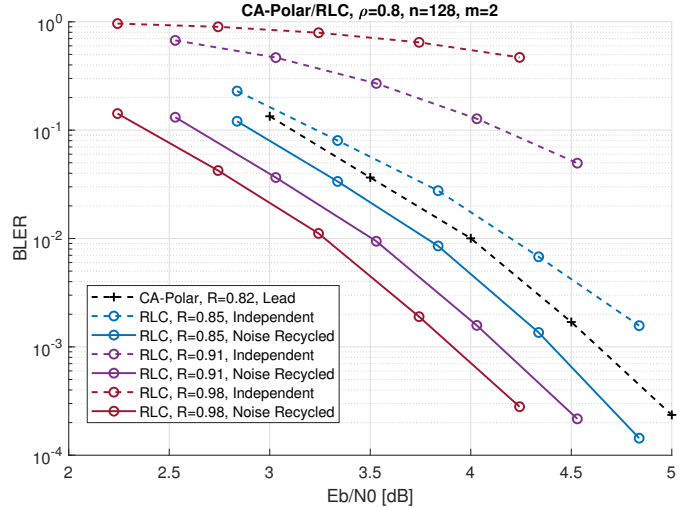


Fig. 8: BLER vs.  $E_b/N_0$  for codes of length  $n = 128$  decoded with ORBGRAND with and without Noise Recycling. Dashed lines correspond to independent decoding, and solid lines to decoding after Noise Recycling. Data on the lead orthogonal channel is encoded with a rate 0.82 CA-Polar code. The second channel uses rate 0.85, 0.91 or 0.98 RLCs.

agation [40], both as implemented in MATLAB’s Communications Toolbox. We also use two soft-information GRAND variants [49], [50], which are well suited to short, high-rate codes. While most decoders are tied to specific codebook constructions, both of these can decode any block code, including CA-Polar codes and RLCs.

##### A. Static Noise Recycling

We first consider a sequential decoding scheme akin to the one described in Section III where a lead channel is selected *a priori* and decoded. A subsequent channel that has a higher rate is then decoded using noise recycled information. Block-errors are counted separately on each channel.

In the first simulation, the lead channel encodes its data using a CA-Polar code [256, 170] with rate  $R_1 \approx 2/3$ . The second, orthogonal channel uses a higher rate CA-Polar code, either [256, 180] or [256, 190] giving  $R_2 \approx 0.7$  or 0.74 respectively. Noise variances are the same on both channels and the noise correlation, which is set to  $\rho = 0.5$ , is known to the second decoder. Both channels are decoded with CA-SCL, with the second channel benefiting from Noise Recycling.

Fig. 7 reports BLER vs  $E_b/N_0$  for these medium length codes. The black dashed line corresponds to the lead channel, while the dashed blue and red lines give the performance curves should Noise Recycling not be used, corresponding to independent decoding of all channels. As the second orthogonal channel runs at a higher rate than the lead channel, if decoded independently the second channel would experience higher BLER than the lead channel. The solid blue and red lines report the performance of the second decoder given noise recycling. Despite using a higher rate code than the lead channel, with Noise Recycling the second channel experiences better BLER vs  $E_b/N_0$  performance. Notably, owing to the better  $E_b/N_0$  (i.e. the energy per **information** bit used in the

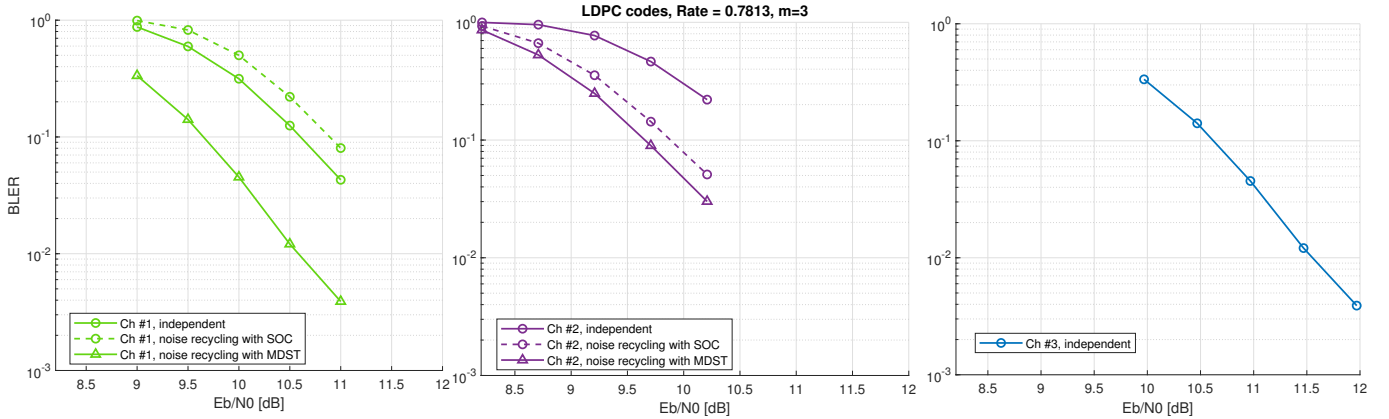


Fig. 9: BLER vs  $E_b/N_0$  for  $[12800, 10000]$  LDPC codes decoded with Belief Propagation and static Noise Recycling, for  $m = 3$  orthogonal channels. The correlation values between the different channels are  $\rho_{1,2} = 0.6$ ,  $\rho_{1,3} = 0.8$ , and  $\rho_{2,3} = 0.4$ . The values of the variance of the orthogonal channels are  $\sigma_1^2 = \sigma_f^2$ ,  $\sigma_2^2 = 1.2 \sigma_f^2$  and  $\sigma_3^2 = 0.8 \sigma_f^2$ . The third channel is chosen as the leading channel, while the order of subsequent channels are chosen statically using either Algorithm 1 (MDST), or a simple sequential orthogonal channel (SOC) order.

transmission) that comes from running a higher rate code, the rate 0.74 code provides better BLER than the rate 0.7 code. For a commonly used target BLER of  $10^{-2}$ , Noise Recycling results in  $\approx 1$  dB gain for the  $[256, 190]$  code.

Fig. 8 reports an analogous simulation for short, high-rate codes, additionally illustrating that the methodology is agnostic to having distinct codes on different channels. With  $\rho = 0.8$ , the lead channel's code is a  $[128, 105]$  CA-Polar code of rate  $R_1 = 0.82$  and the second channel is one of three RLCs with a rate ranging from 0.85 to 0.98. Both channels are decoded with the recently proposed soft detection decoder Ordered Reliability Bits Guessing Random Additive Noise Decoding (ORBGRAND) [50]. As with all the GRAND algorithms, it can decode any code, making it viable for use with RLCs, which encompass all possible codes. A similar phenomenology to the previous figure can be seen, where the impact of Noise Recycling is even more dramatic, allowing the second channel code to use reliably a much higher rate than the lead channel.

Our last simulation of this section illustrates that noise recycling also provides BLER gains for long codes. In Section III we proved that MDST determined an optimal static order for decoding in the presence of asymmetric channel conditions. Here we demonstrate that decoding order plays a significant role in decoding performance for heterogeneous channel conditions.

We simulated Noise Recycling for  $m = 3$  orthogonal channels subject to asymmetric, correlated Gaussian noise, with correlations  $\rho_{1,2} = 0.6$ ,  $\rho_{1,3} = 0.8$  and  $\rho_{2,3} = 0.4$ . We define a common noise factor,  $\sigma_f^2$ , so the noise variance of the channels is given by  $\sigma_1^2 = \sigma_f^2$ ,  $\sigma_2^2 = 1.2 \sigma_f^2$  and  $\sigma_3^2 = 0.8 \sigma_f^2$ . Each channel used a long  $[12800, 10000]$  5G LDPC code, decoded with Belief Propagation, and two static Noise Recycling orders are illustrated. One is the optimal SNR order, as determined by Algorithm 1 (MDST), that is advocated here, which is to lead with Channel 3, then recycle noise before decoding Channel 1, and then recycle again before decoding Channel 2. The other is an order that does

not take the channel conditions into account. It contrast, it again leads with Channel 3, but then recycles noise to Channel 2, before decoding and recycling noise to Channel 1 for its decoding.

Fig. 9 reports BLER performance of these two static orders. As Channel 3, which operates at the best SNR, leads for both orders, it experiences fixed performance. Using MDST then sees a gain of  $\sim 1.25$ dB on Channel 1, followed by a gain of  $\sim 1$ dB on Channel 2. In contrast, in the non-optimal order, while Channel 2 sees a  $\sim 0.75$ dB gain, it is operating at the lowest SNR and the noise that it passes for recycling to Channel 1 is deleterious, leading to  $\sim 0.25$ dB loss. Overall, a  $> 2$ dB gain is possible with MDST, while using an inappropriate order sees a total gain of only 0.5dB.

## B. Dynamic Noise Recycling

While previous sections identified rate and BLER improvements that are available from running a pre-determined lead channel with a lower rate code so that an accurate inference of a noise realization could be obtained to aid the signal at a higher rate second channel, here we consider an alternate design that can lead to a significant additional gain with both short and long codes.

The principle behind Dynamic Noise Recycling is that all orthogonal channels initially attempt to decode their outputs contemporaneously. In principle one would then wish to select the most confident decoding to lead the Noise Recycling for that particular realization. In practice, it may be necessary to use a post-decoding soft-information proxy for that confidence. For example, regardless of the decoders employed, one could select the least energetic estimated noise sequence or the most likely noise sequence. While some decoders, such as those based on the GRAND paradigm, themselves provide soft information on the confidence of their decoding. The Dynamic Noise Recycling decoding procedure with only one round of competition is described in Algorithm 2.

As an example, suppose there are 3 orthogonal channels. At the first step, all decode in parallel. If decoder 2 provides the

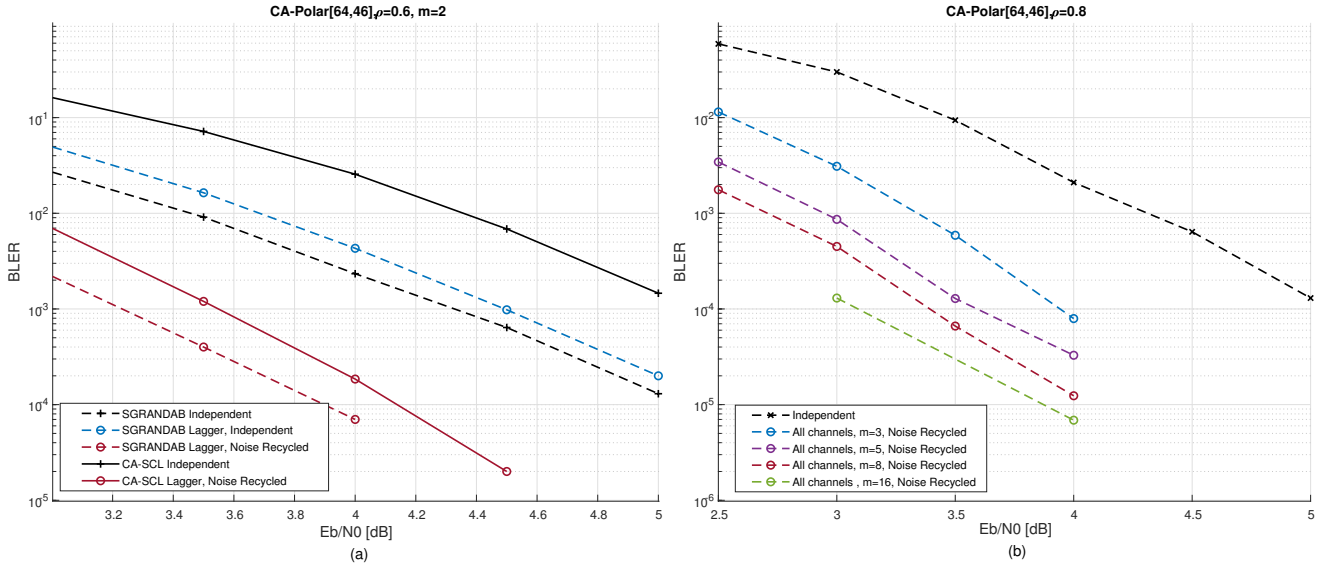


Fig. 10: BLER vs Eb/N0 for [64, 46] CA-Polar codes with dynamic Noise Recycling using SGRANDAB with an abandonment threshold of  $b = 10^6$  for decoding in the first phase. In (a), either SGRANDAB or CA-SCL, which uses a list size of  $L = 32$ , is used to decode the remaining channels after Noise Recycling, while in (b) all decoding is done using SGRANDAB.

---

### Algorithm 2 Dynamic Noise Recycling

---

**Input:**  $\vec{y}_1, \dots, \vec{y}_m$

**Output:**  $\hat{c}_1, \dots, \hat{c}_m$

- 1: Decode orthogonal channel outputs
- 2:  $i \leftarrow \#$  of most confident decoding
- 3:  $\hat{c}_i \leftarrow i$ -th decoded codeword
- 4:  $\hat{x}_i \leftarrow$  modulation of  $\hat{c}_i$
- 5:  $\hat{z}_i \leftarrow \vec{y}_i - \hat{x}_i$
- 6: **for**  $j = 1 \rightarrow \max\{m - i, i - 1\}$  **do**
- 7:   **if**  $i + j \leq m$  **then**
- 8:      $\begin{bmatrix} \hat{c}_{i+j}, \hat{z}_{i+j} \end{bmatrix} \leftarrow \text{DecodeAndEst.}(\vec{y}_{i+j}, \hat{z}_{i+j-1}, i + j - 1, i + j)$
- 9:   **end if**
- 10:   **if**  $i - j \geq 1$  **then**
- 11:      $\begin{bmatrix} \hat{c}_{i-j}, \hat{z}_{i-j} \end{bmatrix} \leftarrow \text{DecodeAndEst.}(\vec{y}_{i-j}, \hat{z}_{i-j+1}, i - j + 1, i - j)$
- 12:   **end if**
- 13: **end for**
- 14: **return**  $\hat{c}_1, \dots, \hat{c}_m$

**procedure** DECODEANDEST.  $(\vec{y}, \hat{z}, i, j)$

$\hat{y} \leftarrow \vec{y} - \rho'_{j,i} \hat{z}$

  Decode orthogonal channel  $j$  using  $\hat{y}$

$\hat{c} \leftarrow$  decoded codeword

$\hat{x} \leftarrow$  modulation of  $\hat{c}$

$\hat{z} \leftarrow \vec{y} - \hat{x}$

**return**  $\hat{c}, \hat{z}$

**end procedure**

---

most accurate decoding, it is selected as the lead, providing an estimate  $\hat{z}_2$  to the decoders 1 and 3, which repeat the process. Note that mixing-and-matching of decoders, even at different stages of the dynamic Noise Recycling, is possible.

We first we consider decoders in which the speed of decoding provides a measure of confidence in their decoding accuracy. Soft GRAND with ABandonment (SGRANDAB) [49] has that feature. SGRANDAB aims to identify the noise that corrupted a transmission from which the codeword can be inferred, rather than identifying the codeword directly and can decode any block code. It does this by removing possible noise effects, from most likely to least likely as determined by soft information, from a received signal and querying whether what remains is in the codebook. The first instance that results in success is a maximum likelihood decoding. If no codeword is found before a given number of codebook queries, SGRANDAB abandons decoding and reports an error. SGRANDAB reports the number of code-book queries made until a code-book element was identified, and fewer queries can be used as a proxy for a more confident decoding.

We simulated Dynamic Noise Recycling in GM channels using a [64, 46] CA-Polar code. We first consider the method on  $m = 2$  orthogonal channels with  $\rho = 0.6$ , where the initial decoding is performed using SGRANDAB on both channels, and the noise-recycled decoding is performed using either SGRANDAB or CA-SCL. Fig. 10 (a) reports BLER performance. As without Noise Recycling SGRANDAB results in lower BLER than CA-SCL, it provides a correct noise sequence more often. The second decoder can use SGRANDAB, as during the initial phase, or instead use CA-SCL. Either way, the remaining channel benefits significantly from Noise Recycling, with a gain of more than 1 dB, even for codes of the same rate, by Dynamic Noise Recycling. Fig. 10 (b) reports the BLER of an SGRANDAB decoded channel



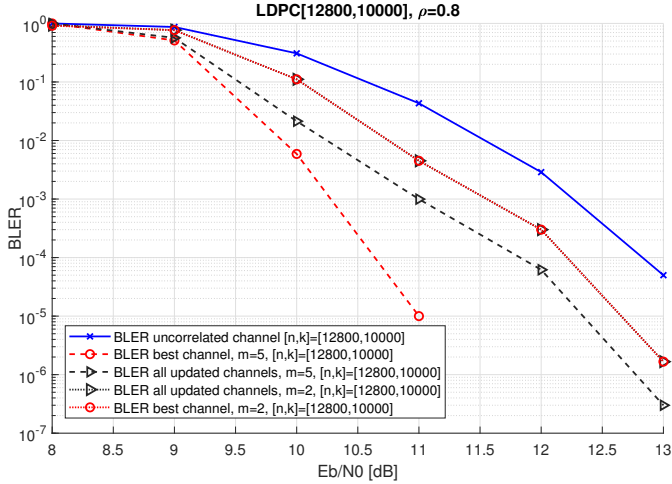


Fig. 11: BLER vs  $E_b/N_0$  for  $[12800, 10000]$  LDPC codes decoded with Belief Propagation and dynamic Noise Recycling in  $m = 5$  and  $m = 2$  channels.

without Noise Recycling. For  $\rho = 0.8$ , and  $m = 3, 5$  or  $8$ , Dynamic Noise Recycling is employed for one round, and then Noise Recycling, where all decoders use SGRANDAB. Again, this shows a significant improvement in BLER for all values of  $m$ . For example there is a gain of about 1.7 dB for  $m = 8$  at a target BLER of  $10^{-4}$ .

We next considered decoders in which the proxy for the most confident decoding could be the channel whose noise estimation is the most likely. Initially the  $i$ -th decoder decodes its orthogonal channel output  $\tilde{y}_i$  without Noise Recycling, and proceeds to compute the log-likelihood of the estimated noise  $\hat{z}_i$ ,

$$l_i(\hat{z}_i; 0, \sigma) = - \sum_{j=1}^n \log \left( \frac{1}{\sigma \sqrt{2\pi}} e^{-\hat{z}_{i,j}^2 / (2\sigma^2)} \right),$$

for each  $i \in \{1, \dots, m\}$ . Using the log-likelihood of the noise estimated at each decoder, the leading decoder is chosen as the decoder with the most likely noise channel estimated, namely,

$$\arg \max_{(i)} l_i(\hat{z}_i; 0, \sigma).$$

The remaining decoders subtract the correlated portion of the estimated noise from their received signals, starting from orthogonal channels  $i \pm 1$ , that leads to higher SNRs, as depicted in Fig. 3.

Fig. 11 provides performance results for  $[12800, 10000]$  LDPCs decoded with Belief Propagation. Even at these long block-lengths, where one might expect noise variability between different channels to average out, a gain of approximately 1.25 dB is observed between a decoder that does not use Noise Recycling, and a decoder that does so with  $m = 5$  at a target BLER of  $10^{-3}$ .

### C. Noise Recycling With Re-Recycling

In all of the results shown so far, the lead channel pays a price by not benefitting from Noise Recycling. Here we demonstrate the potentially counter-intuitive point that this

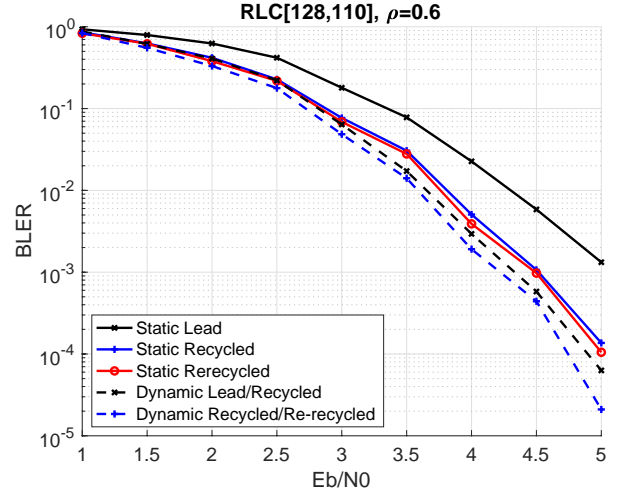


Fig. 12: BLER vs  $E_b/N_0$  for two  $[128, 110]$  RLCs decoded with ORBGRAND and using Static or Dynamic Noise Recycling with and without Re-Recycling for a symmetric Gaussian channel with  $\rho = 0.6$ .

need not be the case. Instead, one can re-recycle, feeding back a recycled noise to the lead channel, redecode it, and get improved BLER. Reconsidering the heuristic argument presented in equation (1), on re-recycling, this block error rate on the left hand side plays the role that  $B(\sigma^2)$  did in the discussion of recycling. As a result, this gives additional probability to the  $B(\sigma^2(1 - \rho^2))$  term and so a further contraction to a less noisy channel, improving the lead channel's decoding.

For a symmetric Gaussian model with two channels employing RLCs decoded with ORBGRAND, Fig. 12 reports BLER performance. For Static Noise Recycling, where a pre-determined channel is chosen to always lead, the black line reports its BLER curve, while the blue line reports the BLER curve of the second channel after Noise Recycling. The noise recycled channel experiences a  $\sim 0.5$ dB gain at a target BLER of  $10^{-3}$ . The red curve provides the BLER performance for the lead channel after Noise Recycling is used from the second channel and it is re-decoded, and its performance slightly outstrips the second channel, also giving a  $\sim 0.5$ dB gain. That is, through Noise Recycling with Re-Recycling, both channels have gained approximately 0.5dB, and the lead channel is at no disadvantage. In dashed lines, also shown are the results for the Dynamic Noise Recycling results with ORBGRAND's query count used as the proxy for decoding confidence. With Dynamic Noise Recycling, each channel is the lead  $\sim 50\%$  of the time and the recycled channel  $\sim 50\%$  of the time, giving the dashed black line. With Re-Recycling, the lead channel is replaced with its re-recycled decoding and a further gain is obtained.

Fig. 13 provides a second example of re-recycling, but with asymmetric channels. Here two channels use the same class of  $[64, 46]$  RLCs, but with channel two having a SNR that is 2dB lower than that experienced on channel one. The solid red and blue lines show the independent BLER curves of each channel when decoded independently. If, as advocated in this paper, MDST was applied to determine a static recycling

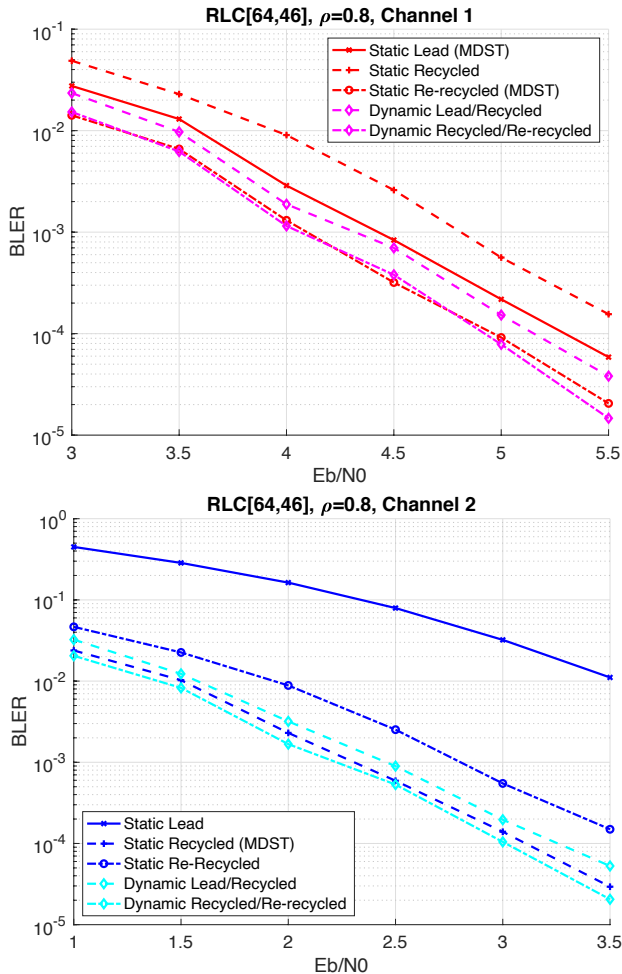


Fig. 13: BLER vs  $E_b/N_0$  for two  $[64, 46]$  RLCs decoded with ORBGRAND and using Static or Dynamic Noise Recycling with Re-Recycling, where channel one is operating at 2dB higher than channel two, and  $\rho = 0.8$ .

order Channel 1 would be selected as the lead. In that case, Channel 1 would have BLER performance of the solid red line and the performance of Channel 2, which benefits from Noise Recycling, would improve to the dashed blue line, a gain of over 2dB. If Re-Recycling was used, Channel 1's performance would see the improvement shown in the dash-dotted red line, giving it a gain of  $\sim 0.5$ dB. That is, by first decoding the more reliable channel, the less reliable channel's performance is improved. However, by Re-Recycling noise, the first channel's performance is then also improved. If MDST was not applied and Channel 2, the less reliable one, was chosen as the lead, due to the asymmetry, the performance of Channel 1 degrades by  $\sim 0.3$ dB after Noise Recycling. This emphasises that in the presence of asymmetries, static order choice has significant consequences. However, even in this case, having chosen Channel 2 as the lead in contradiction to the order determined by MDST, note that its performance is significantly enhanced by Re-Recycling, swapping the solid blue line for the dash-dotted blue one.

When Dynamic Noise Recycling is employed with OR-

BGRAND's query count used as the soft information that determines decoding confidence, each channel is a dynamic mixture of being the lead channel and the recycled one (the dashed magenta and cyan lines) or, if Re-Recycling is used, the recycled channel and the re-recycled channel (the dash-dotted magenta and cyan lines). The performance of these is also shown, where it can be seen that the latter, a dynamically chosen average of being recycled or re-recycled, gives the best performance with an approximate 2dB gain for Channel 2 and a  $\sim 0.5$ dB gain for Channel 1.

## V. CONCLUSION AND DISCUSSION

We introduced Noise Recycling for orthogonal channels experiencing correlated noise, as a means to improve communication performance for any combination of codes and decoders. The performance improvement is twofold, we proved it enables rate gains and provided evidence of its reliability improvement aspect. We analyzed orthogonal correlated channels, i.e. channels in which data that is sent on different channels is independent. A natural extension is considering the use of Noise Recycling in wireless communications, and the consequences of uncertainty in it. Noise Recycling points to the benefit of correlation among orthogonal channels, opening an interesting vein of investigation where orthogonal channels, say in OFDM or TDMA, are chosen with a preference for noise correlation among them, with attendant effects in terms of rate and power allocation among orthogonal channels. In particular, noise correlation may be seen as an added advantage to dense OFDM channel placement, beyond the inherently desirable efficiency in bandwidth use that density entails.

## APPENDIX A ACHIEVABILITY PROOF

*Proof.* To establish Theorem III.2, our coding scheme carries the flavor of [12, Chapter 9.1]. We create  $m$  independent random codebooks such that the  $j$ -th codebook consists of  $2^{nR_j}$  codewords independently drawn from  $\vec{X}^j(1), \dots, \vec{X}^j(2^{nR_j}) \sim \mathcal{N}(0, P_j - \epsilon)$ , where  $R_j < C(P_j / (1 - \rho_j^2) \sigma_j^2)$ , and a superscript  $j$  indicates that a codeword was chosen from the  $j$ -th codebook. For each orthogonal channel, the codebook need only be known at its encoder and decoder. The transmitters of the orthogonal channels send  $\vec{X}^1(i_1), \dots, \vec{X}^m(i_m)$ . The decoders operate according to the decoding order dictated by Lemma III.1. With  $\hat{\vec{Z}}_{\pi(j)} = 0$  if  $\pi(j) = r$ , the  $j$ -th decoder subtracts  $\rho'_j \hat{\vec{Z}}_{\pi(j)}$  from its channel output  $\vec{Y}_j$ , resulting in  $\vec{Y}'_j = \vec{Y}_j - \rho'_j \hat{\vec{Z}}_j$ , where

$$\rho'_j = \begin{cases} \rho'_{\pi(j),j} & \pi(j) \neq r \\ 0 & \pi(j) = r \end{cases}$$

and  $\hat{\vec{Z}}_{\pi(j)}$  is the estimated noise of orthogonal channel  $\pi(j)$ . It then identifies as the decoding the unique codeword that is jointly-typical with  $\vec{Y}'_j$  and satisfies the power constraints. If a codeword does not exist or is not unique, the  $j$ -th decoder decodes in error.

We prove the result using techniques redolent of those in [12, Chapter 9.1]. We bound from below the probability that the jointly decoding  $\vec{X}_1, \dots, \vec{X}_m$  is successful. The event of successfully decoding the  $j$ -th channel and all of its predecessors in the MDST is denoted by  $\mathcal{C}_j$ . The event of successfully decoding all orthogonal channels is denoted by  $\mathcal{C}$ . The event of a decoding failure in the  $j$ -th decoder is denoted by  $\mathcal{E}_j$ . Define the following events:

$$E_{0,j} = \left\{ n^{-1} \sum_i (X^j(i))^2 > P_j \right\},$$

$$E_{i,j} = \{X_j(i), Y'_j \text{ are jointly } \epsilon\text{-typical}\}.$$

Then  $P(\mathcal{C}) = \prod_{j=1}^m P(\mathcal{C}_j | \mathcal{C}_{\pi(j)})$ . From results for a single channel, we know that  $P(\mathcal{C}_j | \mathcal{C}_{\pi(j)}) \geq 1 - 3\epsilon$  when  $\pi(j) = r$  for  $n$  sufficiently large. Without loss of generality, assume that the  $j$ -th transmitter sends the first codeword of the  $j$ -th codebook. We bound  $P(\mathcal{E}_j | \mathcal{C}_{\pi(j)})$ ,  $\pi(j) \neq r$  in a similar fashion to the single case:

$$P(\mathcal{E}_j | \mathcal{C}_{\pi(j)}) \leq$$

$$P(E_{0,j} | \mathcal{C}_{\pi(j)}) + P(E_{1,j}^c | \mathcal{C}_{\pi(j)}) + \sum_{i=2}^{2^{nR_j}} P(E_{i,j} | \mathcal{C}_{\pi(j)}),$$

where the inequality follows from the union bound. For sufficiently large  $n$ ,  $P(E_{0,j} | \mathcal{C}_{\pi(j)}) \leq \epsilon$  by the law of large numbers and  $P(E_{1,j}^c | \mathcal{C}_{\pi(j)}) \leq \epsilon$  by joint typicality. We bound  $P(E_{i,j} | \mathcal{C}_{\pi(j)})$ ,  $i > 1$ :

$$P(E_{i,j} | \mathcal{C}_{\pi(j)}) =$$

$$P(E_{i,j} | X_{\pi(j)}, Y_{\pi(j)}, X_{\pi(\pi(j))}, Y_{\pi(\pi(j))}, \dots) \leq$$

$$P(E_{i,j} | X_{\pi(j)}, Y_{\pi(j)}) \leq 2^{-n(I(X_j; Y_j | X_{\pi(j)}, Y_{\pi(j)}) - R_j - 3\epsilon)}$$

and

$$I(X_j; Y_j | X_{\pi(j)}, Y_{\pi(j)})$$

$$= I(X_j; Y_j | X_{\pi(j)}, X_{\pi(j)} + Z_{\pi(j)}) = I(X_j; Y_j | Z_{\pi(j)})$$

$$= h(X_j | Z_{\pi(j)}) + h(Y_j | Z_{\pi(j)}) - h(X_j, Y_j | Z_{\pi(j)})$$

$$= h(X_j) + h(X_j + \rho'_j Z_{\pi(j)} + \Xi_{\pi(j),j} | Z_{\pi(j)}) -$$

$$h(X_j, X_j + \rho'_j Z_{\pi(j)} + \Xi_{\pi(j),j} | Z_{\pi(j)})$$

$$= h(X_j) + h(X_j + \Xi_{\pi(j),j}) - h(X_j, X_j + \Xi_{\pi(j),j})$$

$$= I(X_j; X_j + \Xi_{\pi(j),j}) = I(X_j; Y'_j)$$

using the fact that  $(X_j, \Xi_{\pi(j),j}) \perp Z_{\pi(j)}$ . Therefore,

$$P(E_{i,j} | X_{\pi(j)}, Y_{\pi(j)}) \leq 2^{-n(I(X_j; Y'_j) - R_j - 3\epsilon)}.$$

Picking  $R_j < I(X_j; Y'_j) - 3\epsilon$  yields  $P(\mathcal{E}_{i,j} | \mathcal{C}_{\pi(j)}) \leq 3\epsilon$ . Ultimately, we get  $P(\mathcal{C}) \geq (1 - 3\epsilon)^m$  which concludes the proof as  $\epsilon$  can be made arbitrarily small.  $\square$

## APPENDIX B UPPER BOUND PROOF

In this section, we derive the proof of Theorem III.3:

$$I(X_j, X_i; Y_j, Y_i)$$

$$= I(X_j, X_i; Y_i) + I(X_j, X_i; Y_j | Y_i)$$

$$= I(X_i; Y_i) + I(X_j; Y_i | X_i) + I(X_j, X_i; Y_j | Y_i)$$

$$\stackrel{(a)}{=} I(X_i; Y_i) + I(X_j, X_i; Y_j | Y_i)$$

$$= I(X_i; Y_i) + I(X_i; Y_j | Y_i) + I(X_j; Y_j | X_i, Y_i)$$

$$\stackrel{(b)}{=} I(X_i; Y_i) + I(X_i; Y_j | Y_i) + I(X_j; Y'_j)$$

$$= I(X_i; Y_i) + h(Y_j | Y_i) - h(Y_j | X_i, Y_i) + I(X_j; Y'_j)$$

$$= I(X_i; Y_i) + h(Y_j | Y_i) - h(X_j + \rho'_{i,j} Z_i + \Xi_j | Z_i)$$

$$+ I(X_j; Y'_j)$$

$$= I(X_i; Y_i) + h(Y_j | Y_i) - h(Y'_j) + I(X_j; Y'_j)$$

$$= I(X_i; Y_i) + h(Y_j) - I(Y_j; Y_i) - h(Y'_j) + I(X_j; Y'_j)$$

$$\stackrel{(c)}{=} I(X_i; Y_i) + h(Y_j)$$

$$+ \frac{1}{2} \log(1 - \tilde{\rho}_{i,j}^2) - h(Y'_j) + I(X_j; Y'_j)$$

$$\stackrel{(d)}{=} \frac{1}{2} \log\left(1 + \frac{P_i}{\sigma_i^2}\right) + \frac{1}{2} \log(2\pi e(P_j + \sigma_j^2))$$

$$+ \frac{1}{2} \log(1 - \tilde{\rho}_{i,j}^2) - \frac{1}{2} \log(2\pi e(P_j + (1 - \rho_{i,j}^2) \sigma_j^2))$$

$$+ \frac{1}{2} \log\left(1 + \frac{P_j}{(1 - \rho_{i,j}^2) \sigma_j^2}\right)$$

$$= \frac{1}{2} \log\left(1 + \frac{P_i}{\sigma_i^2}\right) + \frac{1}{2} \log\left(\frac{P_j + \sigma_j^2}{P_j + (1 - \rho_{i,j}^2) \sigma_j^2}\right)$$

$$+ \frac{1}{2} \log(1 - \tilde{\rho}_{i,j}^2) + \frac{1}{2} \log\left(1 + \frac{P_j}{(1 - \rho_{i,j}^2) \sigma_j^2}\right)$$

where (a) follows since  $I(X_j; Y_i | X_i) = 0$  using the fact that  $\vec{X}_j \perp \vec{Z}_i$ , and the fact that  $X_j$  and  $X_i$  are independent, (b) follows from (3), (c) follows from [12, Example 8.5.1] where  $X \sim \mathcal{N}(0, P)$  and  $Y \sim \mathcal{N}(0, P + \sigma^2)$ , such that

$$\text{cov}(Y_i, Y_j) = E(Y_i Y_j) = E(Z_i Z_j) = \rho_{i,j} \sigma_i \sigma_j,$$

and the mutual information between correlated Gaussian random variables with correlation

$$\tilde{\rho}_{i,j} = \rho_{i,j} \frac{\sigma_i \sigma_j}{\sqrt{(P_i + \sigma_i^2)(P_j + \sigma_j^2)}}$$

is

$$(3) \quad I(Y_j; Y_i) = h(Y_j) + h(Y_i) - h(Y_j, Y_i) = -\frac{1}{2} \log(1 - \tilde{\rho}_{i,j}^2),$$

(d) follows from [12, Theorem 8.6.5], where using the fact that  $X_j$  and  $Z_j$  are independent,

$$h(Y_j) \leq \frac{1}{2} \log(2\pi e(P_j + \sigma_j^2)),$$

with equality if and only if  $X_j \sim \mathcal{N}(0, P_j)$ . This completes the upper bound proof.  $\square$

## REFERENCES

- [1] A. Cohen, A. Solomon, K. R. Duffy, and M. Médard, "Noise Recycling," in *IEEE Int. Symp. Inf. Theory*, 2020.
- [2] R. v. Nee and R. Prasad, *OFDM for Wireless Multimedia Communications*, 1st ed. USA: Artech House, Inc., 2000.
- [3] H. Yang, "A road to future broadband wireless access: MIMO-OFDM-Based air interface," *IEEE Commun. Mag.*, vol. 43, no. 1, pp. 53–60, Jan 2005.
- [4] L. Cimini, "Analysis and Simulation of a Digital Mobile Channel Using Orthogonal Frequency Division Multiplexing," *IEEE Transactions on Communications*, vol. 33, no. 7, pp. 665–675, 1985.
- [5] R. Gallager, "A perspective on multiaccess channels," *IEEE Tran. Inf. Theory*, vol. 31, no. 2, pp. 124–142, March 1985.
- [6] O. Edfors, M. Sandell, J. van de Beek, S. K. Wilson, and P. O. Borjesson, "Channel estimation by singular value decomposition," *IEEE Transactions on Communications*, vol. 46, no. 7, pp. 931–939, 1998.
- [7] B. Yang, K. B. Letaief, R. S. Cheng, and Z. Cao, "Channel estimation for OFDM transmission in multipath fading channels based on parametric channel modeling," *IEEE Trans Commun.*, vol. 49, no. 3, pp. 467–479, 2001.
- [8] P. Hoehner, "TCM on frequency-selective fading channels: a comparison of soft-output probabilistic equalizers," in *IEEE GLOBECOM*, vol. 1, 1990, pp. 376–381.
- [9] Y.-S. Choi, P. J. Voltz, and F. A. Cassara, "On channel estimation and detection for multicarrier signals in fast and selective Rayleigh fading channels," *IEEE Tran. Commun.*, vol. 49, no. 8, pp. 1375–1387, 2001.
- [10] M. Cicerone, O. Simeone, and U. Spagnolini, "Channel Estimation for MIMO-OFDM Systems by Modal Analysis/Filtering," *IEEE Tran. Commun.*, vol. 54, no. 10, pp. 1896–1896, 2006.
- [11] Xiaolong Zhu and Jinyin Xue, "On the Correlation of Subcarriers in Grouped Linear Constellation Precoding OFDM Systems Over Frequency Selective Fading," in *2006 IEEE 63rd Vehicular Technology Conference*, vol. 3, 2006, pp. 1431–1435.
- [12] T. M. Cover and J. A. Thomas, *Elements of information theory*. John Wiley & Sons, 2012.
- [13] R. G. Gallager, *Information theory and reliable communication*. Springer, 1968, vol. 2.
- [14] R. Ahlswede, "Multi-way communication channels," 1971.
- [15] H.-H. J. Liao, *Multiple-access channels*. Ph.D. dissertation, Univ. Hawaii, 1972.
- [16] B. S. Tsybakov, "The capacity of a memoryless Gaussian vector channel," *Problemy Peredachi Informatsii*, vol. 1, no. 1, 1965.
- [17] —, "On the transmission capacity of a discrete-time Gaussian channel with filter," *Problemy Peredachi Informatsii*, vol. 6, no. 2, 1970.
- [18] J. Edmonds, "Optimum branchings," *J Res Natl Bur Stand*, vol. 71, no. 4, pp. 233–240, 1967.
- [19] T. H. Cormen, C. E. Leiserson, R. L. Rivest, and C. Stein, *Introduction to algorithms*. MIT press, 2009.
- [20] I. Nevat and J. Yuan, "Channel Tracking using Pruning for MIMO-OFDM Systems over Gauss-Markov Channels," in *ICASSP*, vol. 3, 2007, pp. 193–196.
- [21] I. Abou-Faycal, M. Médard, and U. Madhow, "Binary adaptive coded pilot symbol assisted modulation over Rayleigh fading channels without feedback," *IEEE Tran. Commun.*, vol. 53, no. 6, pp. 1036–1046, 2005.
- [22] M. Médard and R. G. Gallager, "Bandwidth scaling for fading multipath channels," *IEEE Tran. Inf. Theory*, vol. 48, no. 4, pp. 840–852, 2002.
- [23] S. Akin and M. C. Gursoy, "Training Optimization for Gauss-Markov Rayleigh Fading Channels," in *IEEE ICC*, 2007, pp. 5999–6004.
- [24] W. Chen and R. Zhang, "Kalman-filter channel estimator for OFDM systems in time and frequency-selective fading environment," in *ICASSP*, vol. 4, 2004, pp. iv–iv.
- [25] M. Médard, "The effect upon channel capacity in wireless communications of perfect and imperfect knowledge of the channel," *IEEE Tran. Inf. Theory*, vol. 46, no. 3, pp. 933–946, 2000.
- [26] W. Jakes, *Microwave Mobile Communications*. Wiley & Sons, 1974.
- [27] B. D. Anderson and J. B. Moore, *Optimal filtering*. Courier Corporation, 2012.
- [28] J. Gobien, "On detecting a signal while estimating the spectrum of Gauss-Markov noise (Corresp.)," *IEEE Tran. Inf. Theory*, vol. 23, no. 2, pp. 258–261, 1977.
- [29] A. M. Maras, "Locally optimum Bayes detection in ergodic Markov noise," *IEEE Tran. Inf. Theory*, vol. 40, no. 1, pp. 41–55, 1994.
- [30] R. Brown, "A new look at the Magill adaptive filter as a practical means of multiple hypothesis testing," *IEEE Trans. Circuits Syst*, vol. 30, no. 10, pp. 765–768, 1983.
- [31] D. Magill, "Optimal adaptive estimation of sampled stochastic processes," *IEEE Trans. Autom. Control*, vol. 10, no. 4, pp. 434–439, 1965.
- [32] L. P. B. Christensen, "Minimum symbol error rate detection in single-input channels with Markov noise," in *IEEE SPAWC*, 2005, pp. 236–240.
- [33] A. Kavcic, "Soft-output detector for channels with intersymbol interference and Markov noise memory," in *GLOBECOM*, vol. 1B, 1999, pp. 728–732.
- [34] H. Poor, "Robust matched filters," *IEEE Tran. Inf. Theory*, vol. 29, no. 5, pp. 677–687, 1983.
- [35] I. Tal and A. Vardy, "List decoding of Polar codes," in *IEEE Int. Symp. Inf. Theory*, 2011, pp. 1–5.
- [36] —, "List decoding of Polar codes," *IEEE Tran. Inf. Theory*, vol. 61, no. 5, pp. 2213–2226, 2015.
- [37] E. Arikan, "Channel polarization: A method for constructing capacity-achieving codes," in *IEEE Int. Symp. Inf. Theory*, 2008, pp. 1173–1177.
- [38] —, "Channel polarization: A method for constructing capacity-achieving codes for symmetric binary-input memoryless channels," *IEEE Tran. Inf. Theory*, vol. 55, no. 7, pp. 3051–3073, 2009.
- [39] "3GPP TS 38.212, 5G-NR-Multiplexing and channel coding," [https://www.etsi.org/deliver/etsi\\_ts/138200\\_138299/138212/15.02.00\\_60/ts\\_138212v150200p.pdf](https://www.etsi.org/deliver/etsi_ts/138200_138299/138212/15.02.00_60/ts_138212v150200p.pdf), [Online].
- [40] R. Gallager, "Low-density parity-check codes," *IRE Transactions on information theory*, vol. 8, no. 1, pp. 21–28, 1962.
- [41] —, "The random coding bound is tight for the average code (corresp.)," *IEEE Tran. Inf. Theory*, vol. 19, no. 2, pp. 244–246, 1973.
- [42] K. R. Duffy, J. Li, and M. Médard, "Guessing noise, not code-words," in *IEEE Int. Symp. Inf. Theory*, 2018, pp. 671–675.
- [43] —, "Capacity-achieving Guessing Random Additive Noise Decoding," *IEEE Tran. Inf. Theory*, vol. 65, no. 7, pp. 4023–4040, 2019.
- [44] K. R. Duffy and M. Médard, "Guessing random additive noise decoding with soft detection symbol reliability information," in *IEEE Int. Symp. Inf. Theory*, 2019, pp. 480–484.
- [45] K. Duffy, A. Solomon, K. M. Konwar, and M. Médard, "5G NR CA-Polar Maximum Likelihood Decoding by GRAND," in *Conf. on Inf. Sci. Systems*, 2020.
- [46] K. Niu and K. Chen, "CRC-aided decoding of Polar codes," *IEEE Commun. Letters*, vol. 16, no. 10, pp. 1668–1671, 2012.
- [47] A. Balatsoukas-Stimming, M. B. Parizi, and A. Burg, "LLR-based successive cancellation list decoding of Polar codes," *IEEE Trans. Signal Process.*, vol. 63, no. 19, pp. 5165–5179, 2015.
- [48] X. Liang, J. Yang, C. Zhang, W. Song, and X. You, "Hardware efficient and low-latency CA-SCL decoder based on distributed sorting," in *IEEE GLOBECOM*, 2016, pp. 1–6.
- [49] A. Solomon, K. R. Duffy, and M. Médard, "Soft Maximum Likelihood Decoding using GRAND," in *IEEE Int. Conf. Commun.*, 2020.
- [50] K. R. Duffy, "Ordered Reliability Bits Guessing Random Additive Noise Decoding," *preprint arXiv:2001.00546*, 2020.